Acta Biochimica Polonica

Vol. 52 No. 1/2005

179–194

QUARTERLY

Apoptosis induced by membrane damage in human lymphocytes; effects of arachidonic acid and its photoproducts✪

Zofia Zarębska[1✉], Julia Zielińska[1,2], Igor Zhukov[1] and Włodzimierz Maśliński[3]

[1]*Institute of Biochemistry and Biophysics of the Polish Academy of Sciences, Warszawa,* [2]*Department of Immunology, Faculty of Biology, Warsaw University, Warszawa,* [3]*Department of Pathophysiology & Immunology, Institute of Rheumatology, Warszawa, Poland*

Received: 22 December, 2004; accepted: 01 March, 2005

Key words: apoptosis, arachidonic acid-psoralen photoadduct, human lymphocytes, photochemotherapy, PUVA

The effect of arachidonic acid (AA) combined with UVA irradiation was studied in a model system mimicking phototherapy PUVA (psoralen+UVA) *ex vivo in vitro*. The contribution of damage to the plasma membrane by PUVA was tested on human lymphocytes derived from healthy donors. The effect of arachidonic acid (AA) combined with UVA irradiation was compared with that of a psoralen photoadduct to AA added to the culture. The adduct, obtained photochemically and purified, was characterized by NMR and MS spectrometry as a cycloadduct of psoralen to the vinylene bond of the acid (AA<>PSO).

The reactions of cultured cells, manifested 20 h after treatment by changes in apoptosis and mitochondrial depolarization, were monitored by flow cytometry by tagging lymphocytes with appropriate fluorescent probes. Treatment of lymphocyte suspension within AA doses from 40 to 100 μM gradually induced a shift from Anx-V$^+$ (single positive cells) to late apoptotic, Anx-V$^+$PI$^+$ (double positive cells) in a dose dependent manner. The adduct, AA<>PSO, induced apoptotic changes at a concentration 2–3 times higher than free AA. Combination of psoralen (1 μM) or arachidonic acid (20–120 μM) with UVA irradiation (2–6 J/cm^2) accelerated the

---

✉Correspondence to: Zofia Zarębska, Department of Molecular Biology, Institute of Biochemistry and Biophysics PAS, A. Pawińskiego 5A, 02-106 Warszawa, Poland; phone: (48 22) 592 3335; fax: (48 22) 658 4636; e-mail: zozar@ibb.waw.pl

Abbreviations: AA, arachidonic acid; AA<>PSO, arachidonic–acid–psoralen–photoadduct; Anx-V, annexin V tagged with fluorescein isothiocyanate (FITC); JC-1, 5,5′,6,6′-tetrachloro-1,1′,3,3′-tetraethylbenzimidazolylcarbocyanine iodide; MMP, mitochondrial membrane potential; PI, propidium iodide; PLA2, phospholipase 2; PSO, psoralen; PUVA (psoralen+UVA); UVA, waveband of irradiation, (320–400 nm).

plasma membrane changes in a synergic way. Preliminary studies indicated that changes in the transmembrane potential of mitochondria paralleled the apoptosis when cells were treated by AA alone.

Our findings showed that UVA radiation of lymphocytes in the presence of arachidonic acid, as in the presence of psoralen, enhanced apoptosis of cells in a synergic manner. Thus, PUVA-induced apoptosis may proceed in part by a still undefined signaling pathway(s) triggered in lymphocyte membranes.

Ultraviolet radiation A (320–400 nm) in combination with photosensitizing agents is widely applied to treatment of patients with various skin disorders like psoriasis, vitiligo, and other skin manifested diseases (Pathak & Fitzpatrick, 1992). UV lamps emitting narrow band of UVB radiation (290–320 nm) are also applied for psoriasis treatment (Gordon *et al.*, 1999; Calzavara-Pinton, 1997). In both therapies, UV radiation alone and PUVA (psoralen+UVA), successful treatment is presumably due to the deep penetration of UV rays into the skin, comprising subcutaneous peripheral blood capillaries furnished with leukocytes responsible for the immune balance of the system (Krutmann, 1998). The therapeutic effects of PUVA applied systemically to patients with psoriasis apparently stem from its lethal effect on activated T cells infiltrating skin lesions (Coven *et al.*, 1999). Since the application of a modality of PUVA *ex vivo in vitro*, called extracorporeal photopheresis (ECP-PUVA), it has been revealed that PUVA treatment preferentially accelerates apoptosis of neoplastic T cell clones of blood (Enomoto *et al.*, 1997; Berger *et al.*, 2002; Bladon & Taylor, 2003).

The intricate mechanism of PUVA action is still a matter of research. Initially, the primary PUVA target was thought to be nuclear DNA (Song & Tapley, 1979), subsequently DNA and proteins of lymphocytes (Schmitt *et al.*, 1995), and recently, membrane lipids in skin cells and in skin infiltrating T cells (Zarębska *et al.*, 2000). Although numerous studies had been devoted to the mechanism of beneficial PUVA treatment, no straightforward correlation has been found between the photochemical damage of nuclear DNA inside the cell and the immune response reflected in apoptosis (Godar, 1999a) or the spectrum of cytokines released from the cells (Tokura *et al.*, 2001).

In a system mimicking the ECP-PUVA modality one can test *in vitro* the effects of UVA irradiation in combination with various photosensitizers on apoptosis induced in neoplastic leukocyte lines (Godar, 1999b). In this report, normal human leukocytes originated from human blood (peripheral blood mononuclear cells, PBMC) were treated with UVA alone, and with UVA in combination with additives: psoralen, arachidonic acid or its psoralen photoadduct. For detectable effects, all the treatments applied to a primary PBMC culture were tested at doses exceeding those used in UVA/PUVA therapies (1 μM psoralen and 2–6 J/cm^2 of UVA). Cell viability and apoptosis were followed 20 h after treatment by means of flow cytometry with the aid of the following probes: annexin V tagged with fluorescein isothiocyanate (Anx-V), propidium iodide (PI), and JC-1 (5,5′,6,6′-tetrachloro-1,1′,3,3′-tetraethylbenzimidazolylcarbocyanine iodide). This approach enabled us to show that lymphocytes treated by UVA in the presence of arachidonic acid undergo apoptosis similar to that induced by classic PUVA (psoralen + UVA) in an epidermal cell line (Schindl *et al.*, 1998).

To test the contribution of plasma membrane damage, leukocytes were treated with exogeneous additives, with and without UVA radiation. Arachidonic acid (AA) was chosen as the most powerful agent among other fatty acids interacting with membrane lipids. When AA was added to rat lymphocytes at a concentration of 50 μM, it inhibited [^{3}H]thymidine incorporation more effectively than

linoleic or saturated fatty acids (Calder *et al.*, 1991). At 75 μM AA tested *in situ* on a rat hepatoma cell line induced high reduction in mitochondrial membrane potential, and about twice higher reduction than linoleic acid in contrast to saturated fatty acids which were practically without effect (Bernardi *et al.*, 2002, Fig. 4).

Our previous investigations have shown that freshly isolated, short lived, psoralen fatty acid cyclobutane adducts activate: (1) protein kinase pathway in human platelets, (2) tyrosinase activity enhancing melanin production in human melanocytes in culture and (3) apoptosis in human lymphocytes in culture (Caffieri *et al.*, 1996). Cyclobutane adducts of 8-methoxypsoralen to unsaturated fatty acids were detected in the membrane fraction of human lymphocytes UVA irradiated *in vitro* (Caffieri *et al.*, 1991). In the present studies arachidonic acid psoralen cyclobutane adduct, AA<>PSO, served as a model compound of products formed *in vivo* during PUVA therapy. The aim of present studies was to investigate whether AA and its photoadduct induce apoptosis in cultured human lymphocytes.

The presented findings evidence that arachidonic acid and its cyclobutane adduct with psoralen take part in a still undefined signaling pathway(s) which induces apoptosis in human lymphocytes. The contribution of damage to lecithins or phospholipids in the PUVA induced apoptosis is discussed.

MATERIALS AND METHODS

Isolation and culture of primary human lymphocytes. Peripheral blood mononuclear cells were isolated from 40 ml of blood of thirteen healthy volunteers by a standard procedure. All volunteers gave their consent to venipuncture and testing of their blood sample. Blood withdrawn into heparin solution was centrifuged in a Gradisol gradient (Aqua Medica, Łódź, Poland), washed with phosphate-buffered saline (PBS), spun down and suspended in RPMI 1640 medium (Sigma-Aldrich) supplemented with 2 mM glutamine, 100 U/ml penicillin/streptomycin, 10 mM Hepes buffer, pH 7.4, and 5% fetal calf serum (BioCult). The cells were pelleted, suspended in medium at 10^6 cells/ml, and placed on a 24-well ELISA plate; each sample was supplemented with appropriate additives and filled up with medium to 1 ml. The culture was incubated at 37°C in a humidified atmosphere with 5% CO_2 for about 20 h. Then, the cultured PBMC were removed from the wells, and subsequently stained. All the tests were performed in duplicate, and some controls with untreated cells were done in triplicate, the results are expressed as arithmetic mean.

Staining procedure. Annexin-V-FITC/PI staining was carried out with commercial Anx-V/PI Kit 1018 (Biosource, U.S.A.). Five microliters of each probe was added to cell sample diluted with Binding Buffer: Anx-V diluted 10-fold, and PI (50 μg/ml) – 20-fold. At these dilutions 90% of viable cells remained unstained (Anx-V^-PI^-) in the untreated sample and about 50% of cells became annexin V positive (Anx-V^+) in the sample treated with 100 μM AA. The viability of cells was additionally checked with the trypan blue exclusion test. For determining changes in mitochondrial membrane potential (MMP) was used fluorescent probe JC-1, 5,5′,6,6′-tetrachloro-1,1′,3,3′-tetraethyl-benzimidazolylcarbocyanine iodide (Molecular Probes, Eugene, OR, U.S.A.). The staining with JC-1 was performed by addition of 10 μl of standard solution, 1 mg/ml JC-1 in dimethylsulfoxide to 1 ml of cultured cells, and incubation in the darkness at 37°C for 15 min.

FACS analysis. Cell sample was washed with PBS, incubated in the dark with Anx-V/PI in Binding Buffer for 15 min, and analyzed by FACScalibur (Beckton Dickinson, San Jose, CA, U.S.A.) equipped with 488 nm argon laser. Emission band pass filters were BP 530/30 nm for tagged annexin V and BP 585/42 nm for PI. Usually 20 000 events per

sample were recorded, unless specified otherwise, and analyzed with the Cell Quest program. Population above 200 FSC-H (forward light scatter – height) was gated as intact and damaged lymphocytes, and population of PBMC below 200 FSC-H was excluded as comprising prevalently apoptotic bodies and debris. Monocytes and cell debris, present in the 20 h culture, were excluded from analysis by appropriate gating. The cell population circumscribed in the appropriate gate was further submitted to bivariate analysis into quadrants.

Phototreatment of cells. Samples of about one million cells suspended in 1 ml of medium, plated in ELISA wells, were supplemented with additives in ethanol, within the range of 1–240 μM; the final concentration of ethanol did not exceed 2% in culture medium. After 30 min of incubation, the experimental wells were irradiated, with the adjacent control wells covered with aluminum foil. An Osram HQV125 lamp placed horizontally at a 3.5 cm distance from the plate was cooled in a stream of air from a fan, while the ELISA plate was shielded with a plastic cover and kept on ice to avoid excessive heating. The commercially characterized lamp emitted predominantly at 365.5 nm, with admixture of 6.6% at 334.2 nm and 3.3% at 313 nm. The irradiation intensity was 0.33 J/cm^2 per min as measured by an IL-1500 Radiometer with an SEE 015 UVA-sensitive probe (International Light, MA, U.S.A.). The plastic cover of ELISA plate transmits UV light above 290 nm, with 80% of transmittance at 365 nm and about 60% above 330 nm.

Preparation of photoadduct. The photoadduct of arachidonic acid was obtained according to the procedures used to produce photoadducts of psoralen to lecithin (Zarębska *et al.*, 1998). Briefly, a mixture of AA and PSO at a molar ratio 8 : 1 was irradiated in ethanol with 30 J/cm^2 of UVA in a pyrex tube for 90 min with two HQV125 Osram lamps. After irradiation, the mixture was separated on TLC60 F254 plates (Merck) in hexane/ether/formic acid (50 : 50 : 2, by vol.). One of the 11 resultant spots, with R_F 0.49, located above the psoralen control (R_F 0.38) was eluted with ethanol, purified by millipore filtration (Millex FH13, Sigma). That spot, containing the adduct formed at the highest yield (about 4% of the initial psoralen concentration) was used for molecular characteristics and in the tests with lymphocytes. Subsequent NMR analysis was performed one day after chromatography, and MS within two weeks. The adduct remained stable when kept refrigerated in a dry state as checked by its absorption spectra.

Spectroscopy analysis. Absorption spectra were recorded in ethanol on a Varian Cary 3E spectrophotometer (Australia). NMR analysis was performed with a Varian Unity Plus 500 MHz spectrometer (Varian, Palo Alto, CA, U.S.A.) using methods similar to those previously described (Waszkowska *et al.*, 2000). Linear and two-dimensional NMR spectra were measured by collecting 128 acquisitions for each spectrum, recorded at 25°C. The signal of the solvent $CDCl_3$ (Merck, 99.8%) was taken as internal reference at 7.31 p.p.m. Two-dimensional spectra, COSY (COrrelation SpectroscopY) were made with a resolution of 4096 × 512 for t_2 and t_1, respectively; for TOCSY (TOtal Correlation SpectroscopY) the mixing time was 80 ms (Bax & Davis, 1985). The accuracy of the measurements was ±0.01 p.p.m. for the chemical shifts, compared with the NMR spectra of original psoralen and arachidonic acid as controls.

Mass spectra were performed with Micromass Q-TOF (Quadruple Time of Flight, England) for two separate chromatographic isolates with R_F 0.49. Control mass spectra were those of AA calculated at 305.248 (+1) and detected at 305.278, and of psoralen calculated at 187.039 (+1) and detected at 187.059 average *m/z*.

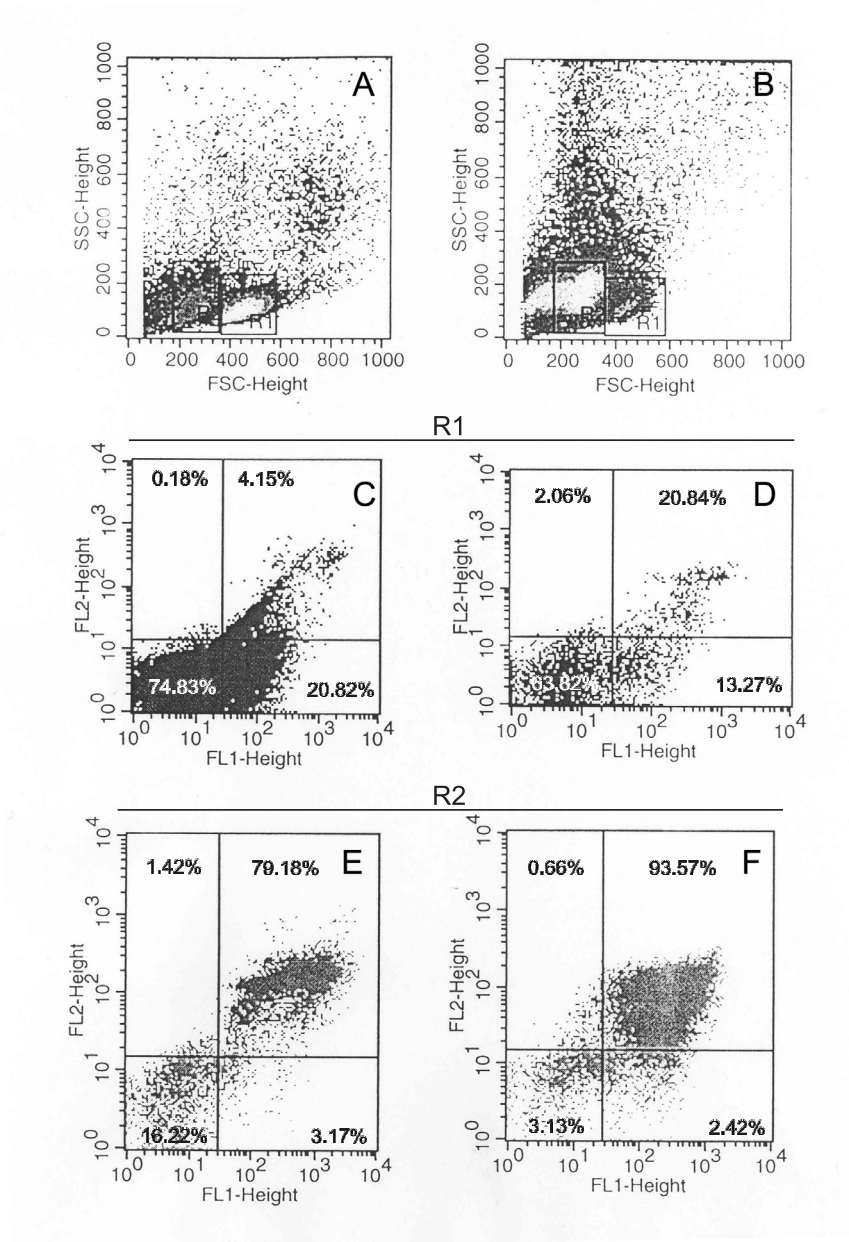

Figure 1. Density plot of light scattering by leukocytes undergoing apoptosis.

Cells were cultured for 23 h and labelled with Anx-V and PI to measure the degree of apoptosis. A, B – Density plot of changes in size (FSC) and granularity (SSC). Anx-V/PI bivariate analysis was presented in quadrants C–F with FL-1 for FITC marker and FL-2 for PI. Left-hand panels A, C, E – are of untreated control; right-hand panels B, D, F – of ones treated with addition of 100 μM AA to the medium. C, D – Distribution of fluorescent probes in gate 1 (R1) and E, F – Distribution of probes in gate 2 (R2) of lymphocyte population (donor YY).

RESULTS

Studies with lymphocytes

The physiological response with regard to apoptosis and transmembrane potential of cells induced by various treatments are presented within Figs. 1–7, each set of results being obtained from a culture of the same donor, indicated in the legend. Analysis of cells derived from thirteen healthy donors gave similar results although with individual variance of donors' response as shown in Fig. 4.

Leukocytes treated with any apoptogenic agent display a typical shift in cytofluorimetric density plots as shown in Fig. 1 (com-

pare with data in Pompéia *et al.*, 2002). The gating circumscribed native and damaged cells and separated debris below 200 FSC-Height. The population of intact cells (Fig. 1A) was split into two subgroups (Fig. 1B), where native cells (R2) were followed by cells undergoing apoptosis (R1), appearing as smaller and more granular ones. The cell populations of both subgroups R1 and R2 were further analyzed by Anx-V/PI bivariate flow cytometry differentiating into quadrants (panels C–F): untagged cells – still native; single positive, Anx-V^+ – early apoptotic, and double positive, Anx-V^+PI^+ – late apoptotic cells. Left-hand panels of Fig. 1 – A, C, E – are of nontreated samples and right-hand panels – B, D, F – are of samples treated with 100 μM of AA. The cell population of the right upper panels D and F (in comparison to panels C and E) discloses an increase of late apoptotic cells to about 15%, in the both subgroups, following treatment with 100 μM AA. However, the subgroup R2 disclosed more pronounced rearrangements of all panels.

The following figures present changes of apoptosis after various combinations of treatments. Figure 2 shows a dose dependent apoptotic shift after treatments with AA alone and its photochemical adduct with psoralen.

Up to 100 μM AA added to the culture, the gradual decrease of cell viability (Fig. 2A) was inversely related to the increase in the number of cells in gate 2 (Fig. 2B). The dose dependent increase was due to incoming early and late apoptotic cells to the gated area. After 24 h of culture, the early apoptotic cells, Anx-V^+, showed a small increment only up to 60 μM AA treatment and then a rapid decrease (Fig. 2C). Increasing the dose of AA above 60–80 μM induced a shift towards late apoptotic cells, Anx-V^+PI^+, as shown in Fig. 2D.

The adduct, AA<>PSO (dashed lines), induced apoptosis at a lower rate than native AA as shown in all panels in Fig. 2. Apoptosis

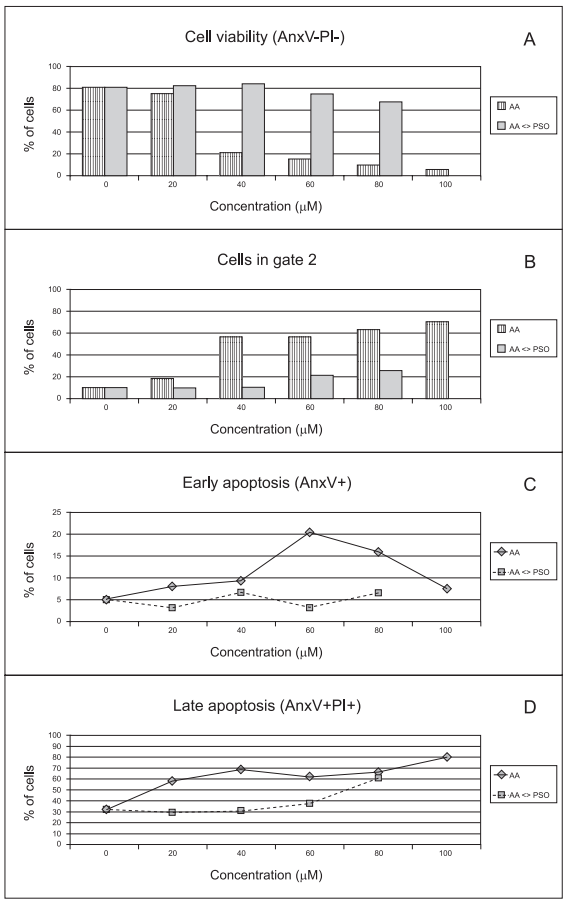

Figure 2. Changes in apoptosis of PBMC treated with AA and its photoadduct AA<>PSO.

Cells were cultured for 24 h and tagged with Anx-V and PI. Fraction of cells in percentage was related to the increasing concentration of additives AA (——) and AA<>PSO (- - -). A – Remaining viable cells in both gates 1 and 2; B – Percentage of all cells in gate 2; C – Early apoptotic cells, labelled with Anx-V^+; D – Late apoptotic cells, double tagged with Anx-V^+ PI^+; C and D were calculated as percentage of cells within gate 2 (donor KL).

induction after adduct treatment was attained at concentrations 2–3 times higher than by arachidonic acid itself. This was confirmed by comparing 50% toxicity of the two agents towards lymphocytes for two other donors (MD, PD, not shown) which were treated with adduct up to 240 μM AA<>PSO. Notably, in Fig. 2 data for 100 μM AA<>PSO treatment, which was not tested with that donor, are missing.

Analysis of apoptosis induced by classic PUVA treatment, 1 μM of PSO plus increas-

ing doses of UVA, is shown in Fig. 3. The gradual decrease of cell viability with the increasing doses of UVA (2–6 J/cm^2) is shown in panel A. The increases in early apoptotic cells (panel B) were more pronounced than changes in the late apoptotic ones (panel C).

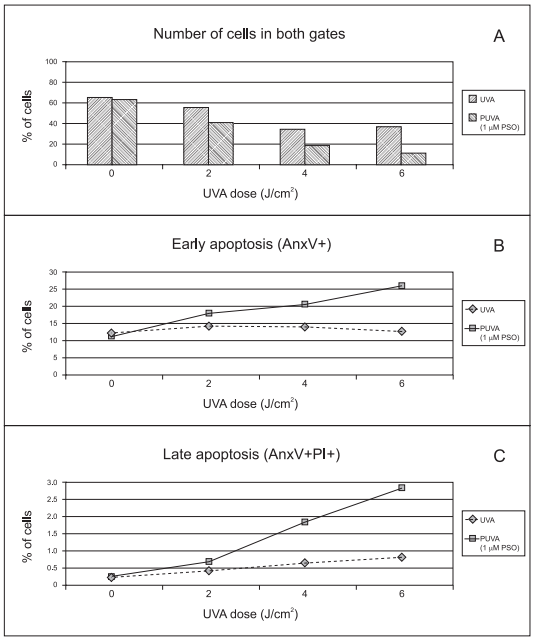

Figure 3. Changes in apoptosis of PBMC induced by UVA/PUVA treatment.

Samples were treated singly by UVA or jointly by 1 μM PSO + 2–6 J/cm^2 of UVA, and analysed at 24 h of culture. A – Number of cells in both gates. B – Cells at early apoptosis; C – cells at late apoptosis; C and D were calculated as percentage of cells within gate 1 (donor MD).

Evidently, UVA irradiation induced additional changes in the presence of psoralen which alone was inert as was checked in control samples. Notably, the changes induced by UVA alone were negligible (dashed lines) whereas those with the combined treatment (full lines) were significant which indicated a synergic action of psoralen and UVA radiation. In analogy, experiments combining AA and UVA treatment were performed (Fig. 4).

In panel A of Fig. 4 the viability curves declined faster under combined treatment of (AA+UVA) than those with AA alone; addition of 1 μM PSO accelerated cell death. The effect of combined treatments was always

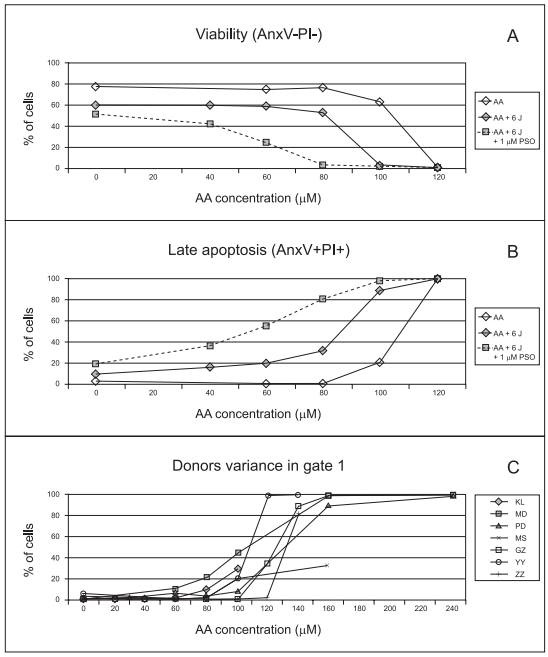

Figure 4. Comparison of combined treatment with AA+UVA or AA+PSO+UVA *versus* treatment with AA alone.

UVA dose was 6 J/cm^2; PSO – 1 μM. Cell population in gate 1 analysed after 23 h of culture. A – Viability; B – Late apoptosis (for panels A and B, donor XX). C – Variance among donors in late apoptotic response due to treatment with AA alone.

stronger than the sum of effects of separate treatments as was checked by appropriate controls. This was shown in the late apoptosis appearance (Fig. 4B) where UVA radiation significantly enhanced the action of AA alone, and an additional increment occurred when PSO and AA were both present in the culture. The accelerated toxicity of AA under UVA radiation and about doubled effect in the presence of PSO indicated synergy of actions.

The inverse shape of curves representing viability and late apoptosis indicated that the increase in the number of late apoptotic cells occurred at the expense of viable cells. The AA-induced toxicity showed considerable variance among donors when analysed by the late apoptosis state (Fig. 4C). For lymphocyte samples coming from the majority of donors 50% viability/toxicity was calculated at 100–120 μM AA, while for adduct treatment 50% viability was around 210 μM AA<>PSO.

The synergism of the combined treatment was revealed when lymphocyte samples (derived of the same donor) were submitted to the three treatments: by AA alone; by AA followed by UVA radiation (AA–>UVA); and by UVA radiation preceding addition of AA (UVA–> AA), as is represented graphically in Fig. 5.

The UVA irradiation, 6 J/cm^2, was the same at various treatments. Bars of panel A representing dead cell changes (loss of viability) show that increments are proportional to AA concentration, gaining plateau at 120 μM AA, but considerably higher when irradiation follows AA addition (AA–>UVA). In the reverse treatment, when irradiation preceded addition of AA, UVA–>AA, the synergy was less evident. Panel B – representing late apoptotic cell increments – showed negative values above 100 μM AA due to a shift of fraction of fragmented apoptotic cells towards a non-gated debris subfraction.

The synergic changes in late apoptosis after combined treatment (AA–> UVA) were compared with the changes in mitochondrial transmembrane potential by alternate staining with the Anx-V/PI and JC-1 probes of samples from the same donor. Density plots and bivariate analysis of lymphocytes treated and stained with JC-1 are exemplified in Fig. 6.

Upon treatment with 100 μM AA there was a shift to gate R2 comprising cells prevalently with collapsed mitochondria (Fig. 6B), similar to the apoptotic shift in the cytograms in Fig. 1B. Further bivariate analysis with JC-1 staining in gate 1 and 2 gave pictures shown in panels 6 C, D and E, F, respectively. Regions 3 of panels C and D contained mainly native cells and regions R4 and R6 of panels E and F – cells with partially or completely collapsed mitochondrial potential. Notably, the changes in the numerical values (% of cells) of regions R4 and R6 of gate 2 (R2) were more significant.

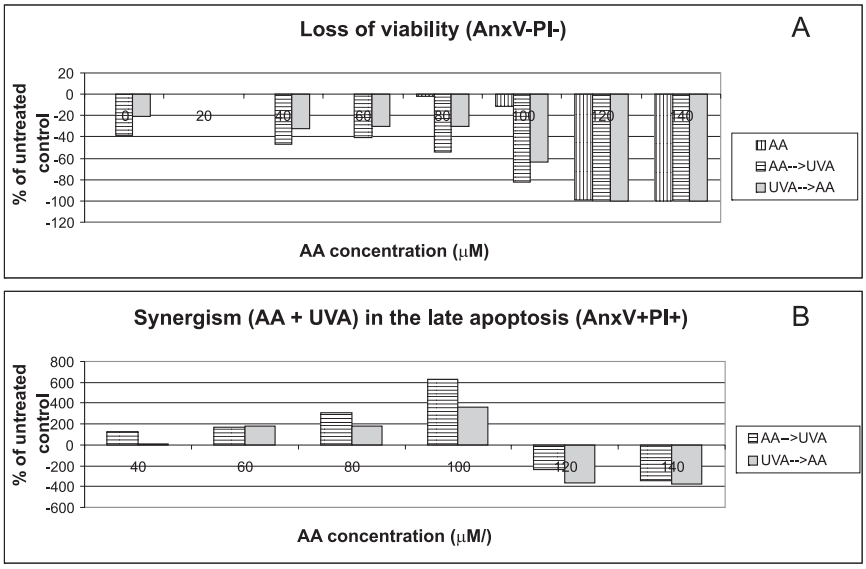

Figure 5. Synergism of combined action of AA and UVA radiation on lymphocytes.

The bars represent percentage of values obtained by combined treatment with (AA–>UVA) or (UVA–> AA) in relation to AA alone. UVA dose was 6 J/cm^2. A – Loss of viability or dead cell increments designated by decreasing values. B – Increments in late apoptosis (donor CC).

The dose relationship of apoptosis (detected by Anx-V/PI) was compared with that of transmembrane potential collapse (detected by JC-1) in Fig. 7. Bivariate analyses of both markers were compared for treated samples, derived from the same donor, and alternatively labelled with Anx-V/PI or JC-1. This was done to verify whether the mitochondrial collapses were in concordance with apoptosis induced by membrane damage.

The numerical values in percentage of JC-1$^+$ cells analysed from regions R6 were compared with the values for late apoptotic cells (Anx-V$^+$PI$^+$). In these preliminary experiments, performed on three subjects, it was found that late apoptotic changes paralleled mitochondrial collapse, whith a steep in-

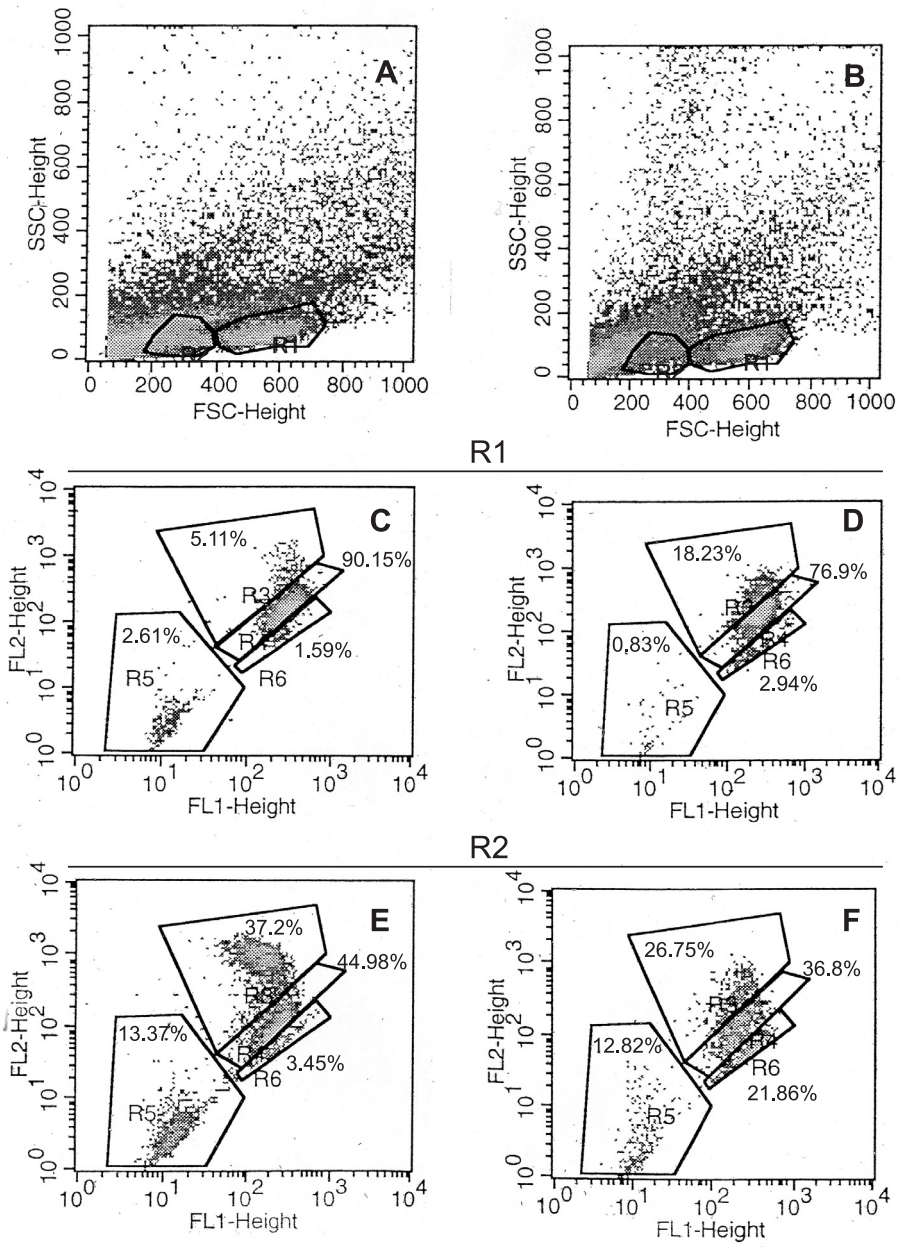

Figure 6. Dot plots of flow cytometric analysis of cells cultured for 21 h and labelled with JC-1.

A, B – changes in size (FSC) and granularity (SSC). Left-sided panels A, C, E – control, nontreated; right-sided panels B, D, F – upon addition of 100 μM AA. Panels C, D were analyzed from gate 1 and panels E, F – from gate 2 populations. Regions 3–5 differentiate JC-1 labelled cells: R3, mainly native cells; R4 and R6 with partially or completely collapsed MMP; R5, debris (donor ZZ).

crease of apoptotic appearance (Anx-V^+PI^+) and MMP (JC-1^+) at 120 μM AA (panel B and A, full line). In contrast, when irradiation accompanied AA treatment, the changes were no longer similar, the percentage of JC-1^+ staining was almost constant while Anx-V^+/PI^+ cells were steadily increasing within the same treatment by 80–140 μM AA (cf. panels A, B, dashed lines). This indicated that the UVA-induced (AA+6 J) mitochondrial mem-

brane collapse proceeds by a different pathway than the outer membrane damage by AA alone.

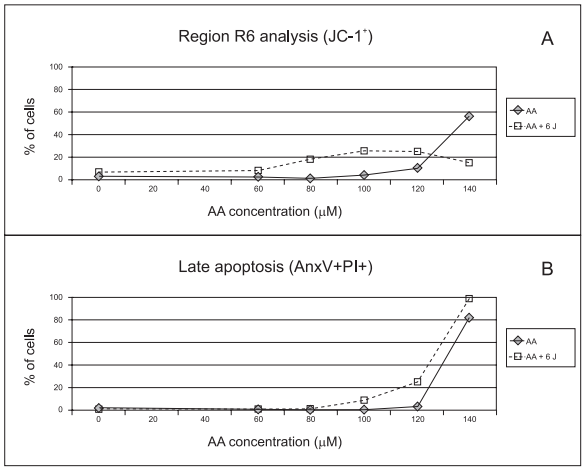

Figure 7. Changes in apoptosis compared to the mitochondrial membrane collapse.

The treated lymphocytes (derived from the same donor) were stained alternatively with Anx-V/PI or JC-1 after 21 h of cell culture and analyzed within population of gate 1. Continuous line for AA alone treatment and dashed line for combined treatment with (AA + 6 J/cm^2 of UVA). The collapse in MMP (cells JC-1$^+$, panel A) was confronted with late apoptotic changes (Anx-V$^+$ PI$^+$), shown in panel B (donor ZZ).

Characteristics of additives to the cell culture

Absorption spectra

Arachidonic acid has a characteristic absorption spectrum in the region of 260–350 nm, with three peaks at 287, 301, 315 nm and a saddle at 260 nm. The other peak, in the far ultraviolet at 196.5 nm, has an absorption coefficient about 850 times higher than the peak at 301 nm (note the concentrations of the measured samples in Fig. 8).

The absorption spectrum of the adduct, AA<>PSO, shows a broad band at 252–259 nm; this band was taken for estimation of adduct concentration with a molar absorption coefficient of 6240 at its maximum; the lower band was at 285 nm, with a saddle at 271 nm. Another peak of the compound at 232 nm with a minimum at 240 nm became clearly visible only after separation by HPLC (not shown). Altogether, the absorption spectrum of AA<>PSO resembled that of psoralen mono-adducts to unsaturated fatty acids, as formerly described (Frank *et al.*, 1998; Zarębska *et al.*, 1998).

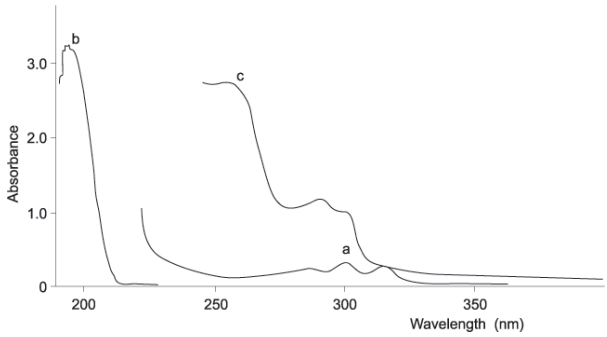

Figure 8. Absorption spectra of native AA and its photoadduct AA<>PSO.

Curve a, with peaks at 287, 301, 315 nm: 2 mg AA per ml ethanol was measured in a 10 mm path length cuvette. Curve b, with a peak at 196.5 nm: 0.225 mg AA per ml ethanol was measured in a 1 mm path length cuvette. Curve c, arachidonic acid-psoralen adduct, AA<>PSO, in ethanol with a large band at 252–259 nm, and a lower band above 285 nm.

Arachidonic acid adduct structure

The arachidonic acid adduct structure was established on the basis of its mass spectra and NMR analysis. Mass spectra of the chromatographic isolates with R_F 0.49 showed a main peak at average *m/z* 491.312 (+1), equal to the sum of AA+PSO estimated at 491.648 (+1); this indicated formation of a mono-adduct of psoralen and arachidonic acid. Fragmented moieties of the adduct were found: PSO at 187.059 (calculated 187.039) and AA at 305.283 *m/z*. The NMR data on all additives to the cell culture are presented in Table 1.

NMR characteristics of the adduct

The proton signals of pyrone ring of adduct, 3H and 4H, moved to the aliphatic part of the spectrum, appearing as signals at *cb*3.40 m and *cb*3.69 m (*cb*, cyclobutane ring). Two

Table 1. NMR data of additives to cell culture: chemical shifts [p.p.m.], shape of signals: s, singlet; d, doublet; t, triplet; q, quartet; m, multiplet.

All spectra recorded in deuterated chloroform, at 25°C. Signals belonging to a cyclobutane ring are preceded by *cb*. The psoralen ring protons are numbered with letter H, while arachidonic acid protons are indicated by sole numbers.

Compound	Psoralen						Arachidonic acid						
	5'H	8H	5H	4'H	4H	3H	vinylenes	2	7, 10, 13 internal edges	4, 16 external flanks	3	$-CH_2-$	$-CH_3$ tail
Psoralen	7.88 d	7.91 s	7.54 s	6.98 d	8.08 d	6.39 d							
AA							5.45 m	2.42 t	2.89 m	2.10 2.20 q	1.78 q	1.40 m	0.95 t
AA<>PSO	7.66 d	7.26 t	7.037 7.025 s	6.75 d	*cb*3.69 m	*cb*3.40 m	5.40, 5.55, 5.15 (all m) *cb* 2.45 m *cb* 2.18 m	2.60 q	2.40 2.90 m	2.06 2.10 m	1.65 m	1.3 m	0.92 m

vinylene protons out of eight were lost in the acid indicating attachment of one vinylene bond. A shift around 2.89 p.p.m. indicated changes in the internal flanking protons, $-CH_2-$, positioned at C 7,10,13 of the intact fatty acid. That signal was decreased to two protons out of six, and a new signal with four protons was shifted upfield to 2.40 p.p.m. Signals of the external flanking protons $-CH_2-$ of C4 and C16 were slightly shifted upfield at 2.10 m and 2.07 m, respectively, and showed an asymmetric enlargement; a new adjacent signal appeared at *cb* 2.18 m in vicinity, originating from cyclobutane ring (vinylene ridge). That new *cb* signal, accompanied by changes in the internal flanking protons of C7 and C10, indicated saturation of the 8==9 vinylene bond.

The signals of the adduct appearing between 3.8 and 2.1 p.p.m. were assigned to a cyclobutane ring including the 3–4 bonding of the pyrone ring, and 8–9 of the vinylene bond, and this was further confirmed by TOCSY experiments. TOCSY spectra indicated couplings of attached PSO: 7.65→6.74→7.26 [5′H→4′H→8H]. The cyclobutane ring was represented by two patterns of cross-peaks: one at 3.69→3.40→2.45→2.18 [4H→3H→9H→8H], and the other at 3.69→3.40→2.58→2.18 [4H→3H→8H→9H].

The changes in the vinylene protons between 5.15–5.55 p.p.m., taken together with multiple peaks of 5H (doublet) and 8H (triplet) of the PSO moiety (see Table 1), and two patterns of cross-peaks of the cyclobutane ring indicated that two isomeric forms of the adduct were present in the eluted sample (chromatographic isolate at R_F 0.49).

Based on our previous studies on the photochemical attachment of PSO to linoleic acid (Zarębska *et al.*, 1998), the above data justified the following formula of the adduct AA<>PSO, appearing in two isomeric forms (Fig. 9). The cyclobutane attachment of PSO to the vinylene bond of AA appears at: $C3^{PSO}$–$C4^{PSO}$–$C8^{AA}$–$C9^{AA}$ and $C4^{PSO}$–$C3^{PSO}$–$C8^{AA}$–$C9^{AA}$, with the psoralen moiety directed towards AA-head or AA-tail, respectively (Frank *et al.*, 1998). The chromatographic system applied in our procedure did

not separate the two isomers of the adduct; hence, the leukocytes were treated with a mixture of the two isomers.

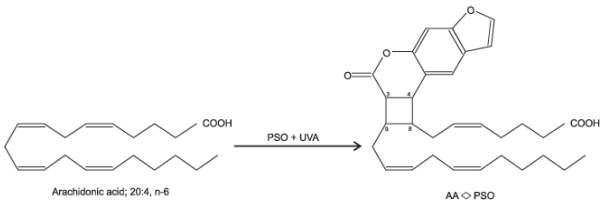

Figure 9. Adduct structure: AA<>PSO, PSO→AA head.

The adduct formula was based on NMR and MS analyses, for details see text and data of Table 1.

DISCUSSION

Toxicity level of AA

In our experiments, AA was estimated to be toxic at 100 – 120 μM (average for lymphocytes from eight donors) as was inferred from the late apoptosis response, after 20 h. The toxicity threshold of combined treatment with (AA–>UVA) was somewhat lower, below 100 μM AA. In the reverse experiments with UVA radiation preceding addition of AA the synergic action was less evident. This might indicate that under UVA radiation membrane damage is induced by AA photoproducts, additionally to AA alone.

Exogeneous AA

Exogeneous AA added to cultures of lymphocytes in our experiments only slightly exceeded the concentration of individual fatty acids in the plasma *in vivo*. In rat plasma AA was estimated to be 30–130 μM in fed animals, and 50–600 μM in exercised, fasted or stressed states (Calder *et al.*, 1991). Free AA in the plasma of humans, non esterified and unbound to albumins, fluctuated between 5.8 and 49.3 μM as cited by Pompéia *et al.* (2002). Those author's findings indicate that exogenously added and internalised AA is incorporated into phospholipids prior to inducing DNA fragmentation and a cascade of apoptosis.

Variation in viability/toxicity

The effect of AA upon primary leukocytes from healthy donors was not uniform. The variation of values in 50% viability of lymphocytes (100 to 120 μM AA) reported here probably reflects the presence of various fractions of cells with different sensitivities to AA. The study of Pompéia and coworkers (2002) on neoplastic cell lines in culture at 5×10^5 cells/ml showed 50% viability in the range of 82–116 μM AA. Interestingly, primary lymphocytes were shown to be more sensitive than Jurkat lymphoma cells to a combined drug and UVA treatments in the presence of 8-MOP, CPZ and TMA (see Wolnicka-Głubisz *et al.*, 2002).

Photoadduct of AA

The approximately twice lower effect of the photoadduct, AA<>PSO, than of free AA may stem from the difference in their lipophilic affinity and limited transport inside the cell. Oxygenated forms of AA or of its adduct AA<>PSO may additionally contribute to the apoptotic pathway(s) initiated in lipids. With a sensitive gas chromatography-MS assay, it was possible to detect 5-hydroxyeicosatetraenoic acid (5-HETE) in plasma of patients submitted to PUVA (8-MOP+UVA), which compound constituted 80% of all HETE isomers (Wiswedel *et al.*, 2000).

Plasma membrane damage and apoptosis

Accumulating evidence suggests that in addition to the apoptosis triggered by damage to nuclear DNA, damage to the cell membranes play a role in induction of apoptosis. Although our studies do not elucidate a direct link between reactions in the plasma membrane and apoptosis or the collapse of the

transmembrane potential of lymphocytes – one can visualize two directions for future studies, discussed below: 1st – release of AA from phospholipids due to the combined action of UVA radiation and psoralen; 2nd – UV-irradiated phosphatidylcholine may be transformed into a derivative of platelet-activating factor (PAF), a molecular sensor for cellular damage, which may act as a PAF-like receptor agonist.

Release of AA by activation of a phospholipase (PLA2) pathway following UVA radiation has been shown in mouse fibroblasts. Irradiation by UVA (2.5–10 J/cm^2) activated PLA2 which in turn induced the release of [^{3}H]-AA from cell lysates into the medium (Cohen & De Leo, 1993). The peak of AA release was noted 4 hours after irradiation, which supported the idea of PLA2 activation by UVA action. The release of [^{14}C]-AA from a culture of human keratinocytes (NCTC 2544) was observed at a dose as low as 2.5 J/cm^2 of UVA; AA released to the medium effected cell death, detectable by trypan blue (TB) test; the TB$^+$ cell number increased after 24 h in comparison with 0.5 h after irradiation (Punnonen *et al.*, 1991).

There is still a matter of debate whether cell membrane damage or mitochondrial damage are the causative agents for apoptosis induction upon AA treatment. Our preliminary studies indicate that both targets are involved. The mechanism of apoptosis studied in clonal hepatoma rat cells showed that arachidonic acid released by PLA2 activation triggered apoptosis through the mitochondrial pathway (Penzo *et al.*, 2004). Jurkat cells treated in serum free medium by PUVA (50 μM PSO + 1.8 J/cm^2) and by irradiated psoralen alone, also indicated mitochondrial membrane collapse as responsible for apoptosis (Canton *et al.*, 2002). However, in our investigations the cells were treated with AA and PSO additives in medium containing 5% calf serum, aiming to be closer to the conditions *in vivo* (Pompéia *et al.*, 2002). Apoptosis inducing a signal transduction pathway alternatively to the mitochondrial pathway may be considered.

Recently, it has been shown in studies on mice that UV-induced platelet-activating factor (PAF) activates cytokine synthesis and initiates UV-induced immune suppression (Walterscheid *et al.*, 2002). A phospholipid proinflammatory mediator that participates in the PUVA-induced immunosuppression was inferred from *ex vivo* UV-irradiated phosphatidylcholine (by means of 270-390 nm emitting lamps), and then injected into mice (Nghiem *et al.*, 2002). It was further postulated that the PAF pathway may be involved in PUVA-induced immune suppression (Wolf *et al.*, 2003, unpublished data).

Our findings, showing an enhanced effect of cell damage after addition of (AA+PSO) and UVA, support the concept that PUVA-induced apoptosis may be initiated by release of AA from lymphocyte phospholipids. In turn, released AA becomes an apoptogenic agent towards adjacent cells. Undoubtedly, the concept of apoptosis induced by a signaling pathway through the cell membrane damage requires further studies.

The *in vivo* metabolism of arachidonic acid, relevant to this investigation, was a subject of intensive research (Wolf & Laster, 1999). AA and its metabolites, the leukotrienes LTB4 and LTD4, were considered to be cellular toxins in neuronal apoptosis in HIV disease; culturing HIV-1 infected monocytes with glia cells stimulated the synthesis of AA and its metabolites, LTB4, LTD4, and PAF, leading to injury of neurons present in the culture. An increased release of AA was postulated to be induced by activated PLA2 (Nath, 2001). It was found that AA converts glutathione depletion-induced apoptosis to necrosis by promoting lipid peroxidation and reducing caspase-3 activity in rat glioma cells (Higuchi & Yoshimoto, 2002). AA-induced apoptosis was connected with oxidative stress accompanied by glutathione depletion (Vento *et al.*, 2000).

All the data discussed above suggest that whatever the cause of AA release to the medium, the released AA combined with UVA radiation contributes to apoptosis triggered in cell membranes. The synergic action of AA and UVA radiation suggests that besides free AA, arachidonic acid photoproducts also induce apoptosis.

In conclusion, our findings establish that treatment with arachidonic acid and psoralen combined with UVA radiation contribute to lymphocyte induced apoptosis. These model experiments are relevant to the mechanism of PUVA action in the human organism.

The authors are indebted to Dr. Nadzieja Drela, supervisor of J.Z. Thesis, for invaluable help and critical reading of the manuscript. Anna Ostapkowicz (M.Sc., 2000, IBB PAS, Warszawa) and Magdalena Legat (M.Sc., 2002, IBB PAS, Warszawa) are appreciated for their participation in the initial phases of this project.

REFERENCES

Bax A, Davis DG. (1985) MLEV-17 based two-dimensional homonuclear magnetization transfer spectroscopy. *J Magn Reson.*; **65**: 355–60.

Berger CL, Hanlon D, Kanada D, Girardi M, Edelson RL. (2002) Transimmunization, a novel approach for tumor immunotherapy. *Transfus Apheresis Sci.*; **26**: 205–16.

Bernardi P, Penzo D, Wojtczak L. (2002) Mitochondrial energy dissipation by fatty acids. Mechanisms and implications for cell death. *Vitam Horm.*; **65**: 97–126.

Bladon J, Taylor PC. (2003) Treatment of cutaneous T cell lymphoma with extracorporeal photopheresis induces Fas-ligand expression on treated T cells, but does not suppress the expression of co-stimulatory molecules on monocytes. *J Photochem Photobiol B: Biol.*; **69**: 129–38.

Caffieri S, Zarębska Z, Dall'Acqua F. (1991) Membrane lymphocyte damage by 8-methoxy-psoralen and UVA radiation. *Méd Biol Environ.*; **19**: 45–50.

Caffieri S, Zarębska Z, Dall'Acqua F. (1996) Psoralen photosensitization: damages to nucleic acid and membrane lipid components. *Acta Biochim Polon.*; **43**: 241–6.

Calder PC, Bond JA, Bevan SJ, Hunt SV, Newsholme EA. (1991) Effect of fatty acids on the proliferation of concanavalin A-stimulated rat lymph node lymphocytes. *Int J Biochem.*; **23**: 579–88.

Calzavara-Pinton PG. (1997) Efficacy and safety of stand-up irradiation cubicles with UVA metal-halide lamps (and a new filter) or UVA fluorescent lamps for photochemotherapy of psoriasis. *Dermatology.*; **195**: 243–7.

Canton M, Caffieri S, Dall'Acqua F, Di Lisa F. (2002) PUVA-induced apoptosis involves mitochondrial dysfunction caused by the opening of the permeability transition pore. *FEBS Lett.*; **522**: 168–72.

Cohen D, De Leo VA. (1993) Ultraviolet radiation-induced phospholipase A_2 activation occurs in mammalian cell membrane preparations. *Photochem Photobiol.*; **57**: 383–90.

Coven TR, Walters IB, Cardinale I, Krueger JG. (1999) PUVA-induced lymphocyte apoptosis: mechanism of action in psoriasis. *Photodermatol Photoimmunol Photomed.*; **15**: 22–7.

Enomoto DNH, Schellekenes PTA, Yong S-L, ten Berge IJM, Mekkes JR, Bos JD. (1997) Extracorporeal photochemotherapy (photopheresis) induces apoptosis in lymphocytes: a possible mechanism of action of PUVA therapy. *Photochem Photobiol.*; **65**: 177–80.

Frank S, Caffieri S, Raffaelli A, Vedaldi D, Dall'Acqua F. (1998) Characterisation of psoralen-oleic acid cycloadducts and their possible involvement in membrane photodamage. *J Photochem Photobiol B: Biol.*; **44**: 39–44.

Godar DE. (1999a) Light and death: photons and apoptosis. *J Invest Dermatol Proc.*; **4**: 17–23.

Godar DE. (1999b) UVA1 radiation triggers two different final apoptotic pathways. *J Invest Derm.*; **112**: 3–12.

Gordon PM, Diffey BL, Matthews JN, Farr PM. (1999) A randomized comparison of narrow band TL-01 phototherapy and PUVA photochemotherapy for psoriasis. *J Am Acad Dermatol.*; **41**: 728–32.

Higuchi Y, Yoshimoto T. (2002) Arachidonic acid converts the glutathione depletion-induced apoptosis to necrosis by promoting lipid peroxidation and reducing caspase-3 activity in rat glioma cells. *Arch Biochem Biophys.*; **400**: 133–40.

Krutmann J. (1998) Therapeutic photoimmunology: photoimmunological mechanisms in photo(chemo)therapy. *J Photochem Photobiol B: Biol.*; **44**: 159–64.

Nath A. (2001) Apoptosis in HIV disease pathogenesis. In *Programmed Cell Death II. Role in Disease, Pathogenesis and Prevention.* Mattson MP, Estus S, Rangnekar VM, eds. pp 101–36. Elsevier Science, Amsterdam.

Nghiem DX, Walterscheid JP, Kazimi N, Ullrich SE. (2002) Ultraviolet radiation-induced immunosuppression of delayed-type hypersensitivity in mice. *Methods.*; **28**: 25–33.

Pathak MA, Fitzpatrick TB. (1992) The evolution of photochemotherapy with psoralens and UVA (PUVA): 2000 BC to 1992 AD. *J Photochem Photobiol B: Biol.*; **14**: 3–22.

Penzo D, Petronilli V, Angelin A, Cusan C, Colonna R, Scoranno L, Pagano F, Prato M, Di Lisa F, Bernardi P. (2004) Arachidonic acid released by phospholipase A2 activation triggers Ca^{2+}-dependent apoptosis through the mitochondrial pathway. *J Biol Chem.*; **279**: 25219–25.

Pompéia C, Freitas JJS, Kim JS, Zyngier SB, Curi R. (2002) Arachidonic acid cytotoxicity in leukocytes: implications of oxidative stress and eicosanoid synthesis. *Biol Cell.*; **94**: 251–65.

Punnonen K, Jansen CT, Puntala A, Ahotupa M. (1991) Effects of *in vitro* UVA irradiation and PUVA treatment on membrane fatty acids and activities of antioxidant enzymes in human keratinocytes. *J Invest Dermatol.*; **96**: 255–9.

Schindl A, Klosner G, Hönigsmann H, Jori G, Calzavara-Pinton PG, Trautinger F. (1998) Flow cytometric quantification of UV-induced cell death in a human squamous cell carcinoma-derived cell line: dose and kinetic studies. *J Photochem Photobiol B: Biol.*; **44**: 97–106.

Schmitt IM, Chimenti S, Gasparro FP. (1995) Psoralen-protein photochemistry — a forgotten field. *J Photochem Photobiol B: Biol.*; **27**: 101–7.

Song PS, Tapley KJ. (1979) Photochemistry and photobiology of psoralens. *Photochem Photobiol.*; **29**: 1177–97.

Tokura Y, Seo N, Yagi H, Takigawa M. (2001) Photoactivational cytokine-modulatory action of 8-methoxypsoralen plus ultraviolet A in lymphocytes, monocytes, and cutaneous T cell lymphoma cells. *Ann N Y Acad Sci USA.*; **941**: 185–93.

Vento R, D'Alessandro N, Giuliano M, Lauricella M, Carabillò M, Tesoriere G. (2000) Induction of apoptosis by arachidonic acid in human retinoblastoma Y79 cells: involvement of oxidative stress. *Exp Eye Res.*; **70**: 503–17.

Walterscheid JP, Ullrich SE, Nghiem DX. (2002) Platelet-activating factor, a molecular sensor for cellular damage, activates systemic immune suppression. *J Exp Med.*; **195**: 171–9.

Waszkowska E, Zarębska Z, Poznański J, Zhukov I. (2000) Spectroscopic detection of photoproducts in lecithin model system after 8-methoxypsoralen plus UV-A treatment. *J Photochem Photobiol B: Biol.*; **55**: 145–54.

Wiswedel I, Bohne M, Hirsch D, Kuhn H, Augustin W, Gollnick H. (2000) A sensitive gas chromatography-mass spectrometry assay reveals increased level of monohydroxyeicosatetraenoic acid isomers in hu-

man plasma after extracorporeal photoimmunotherapy and under *in vitro* ultraviolet A exposure. *J Invest Dermatol.*; **115**: 499–503.

Wolf LA, Laster SM. (1999) Characterization of arachidonic acid-induced apoptosis. *Cell Biochem Biophys.*; **30**: 353–68.

Wolnicka-Głubisz A, Rijnkels JM, Sarna T, Beijersbergen van Henegouwen GMJ. (2002) Apoptosis in leukocytes induced by UVA in the presence of 8-methoxypsoralen, chlorpromazine or 4,6,4′-trimethylangelicin. *J Photochem Photobiol B: Biol.*; **68**: 65–72.

Zarębska Z, Waszkowska E, Caffieri S, Dall'Acqua F. (1998) Photoreactions of psoralens with lecithins. *J Photochem Photobiol B: Biol.*; **45**: 122–30.

Zarębska Z, Waszkowska E, Caffieri S, Dall'Acqua F. (2000) PUVA (psoralen+UVA) photochemotherapy: processes triggered in the cells. *Il Farmaco.*; **55**: 515–20.